PLOS GENETICS

RESEARCH ARTICLE

Molecular basis of hemoglobin adaptation in the high-flying bar-headed goose

Chandrasekhar Natarajan[1], Agnieszka Jendroszek[2], Amit Kumar[1], Roy E. Weber[2], Jeremy R. H. Tame[3], Angela Fago[2], Jay F. Storz[1]*

1 School of Biological Sciences, University of Nebraska, Lincoln, NE, United States of America, **2** Department of Bioscience, Zoophysiology, Aarhus University, Aarhus, Denmark, **3** Drug Design Laboratory, Graduate School of Medical Life Science, Yokohama City University, 1-7-29 Suehiro, Yokohama, Kanagawa, Japan

* jstorz2@unl.edu

OPEN ACCESS

Citation: Natarajan C, Jendroszek A, Kumar A, Weber RE, Tame JRH, Fago A, et al. (2018) Molecular basis of hemoglobin adaptation in the high-flying bar-headed goose. PLoS Genet 14(4): e1007331. https://doi.org/10.1371/journal.pgen.1007331

Editor: Jianzhi Zhang, University of Michigan, UNITED STATES

Received: January 22, 2018

Accepted: March 23, 2018

Published: April 2, 2018

Data Availability Statement: All relevant data are within the paper and its Supporting Information files.

Funding: This work was funded by the National Institutes of Health/National Heart, Lung, and Blood Institute (HL087216 to JFS), the National Science Foundation (MCB-1517636 and RII Track-2 FEC-1736249 to JFS), OpenEye Scientific Software to JRHT, and the Danish Council for Independent Research, Natural Sciences (4181-00094 to AF). The funders had no role in study design, data

Abstract

During the adaptive evolution of a particular trait, some selectively fixed mutations may be directly causative and others may be purely compensatory. The relative contribution of these two classes of mutation to adaptive phenotypic evolution depends on the form and prevalence of mutational pleiotropy. To investigate the nature of adaptive substitutions and their pleiotropic effects, we used a protein engineering approach to characterize the molecular basis of hemoglobin (Hb) adaptation in the high-flying bar-headed goose (*Anser indicus*), a hypoxia-tolerant species renowned for its trans-Himalayan migratory flights. To test the effects of observed substitutions on evolutionarily relevant genetic backgrounds, we synthesized all possible genotypic intermediates in the line of descent connecting the wildtype bar-headed goose genotype with the most recent common ancestor of bar-headed goose and its lowland relatives. Site-directed mutagenesis experiments revealed one major-effect mutation that significantly increased Hb-O_2 affinity on all possible genetic backgrounds. Two other mutations exhibited smaller average effect sizes and less additivity across backgrounds. One of the latter mutations produced a concomitant increase in the autoxidation rate, a deleterious side-effect that was fully compensated by a second-site mutation at a spatially proximal residue. The experiments revealed three key insights: (*i*) subtle, localized structural changes can produce large functional effects; (*ii*) relative effect sizes of function-altering mutations may depend on the sequential order in which they occur; and (*iii*) compensation of deleterious pleiotropic effects may play an important role in the adaptive evolution of protein function.

Author summary

During adaptive phenotypic evolution, some of the associated genetic changes may contribute directly to changes in the selected trait (causative mutations) and other changes may ameliorate the negative side-effects of the causative changes (compensatory mutations). To assess the nature of such changes and their relative prevalence, we used a protein engineering approach to characterize the molecular basis of a well-documented

collection and analysis, decision to publish, or preparation of the manuscript.

Competing interests: The authors have declared that no competing interests exist.

biochemical adaptation: the increased hemoglobin-oxygen affinity in the bar-headed goose (*Anser indicus*), a champion of high-altitude flight. The experiments revealed the contributions of specific substitutions to the adaptive increase in hemoglobin-oxygen affinity in bar-headed goose and demonstrated that compensatory interactions may play an important role in adaptive protein evolution due to trade-offs between different functional properties.

Introduction

During the adaptive evolution of a given trait, some of the selectively fixed mutations will be directly causative (contributing to the adaptive improvement of the trait itself) and some may be purely compensatory (alleviating problems that were created by initial attempts at solution). Little is known about the relative contributions of these two types of substitution in adaptive phenotypic evolution and much depends on the prevalence and magnitude of antagonistic pleiotropy [1–9]. If mutations that produce an adaptive improvement in one trait have adverse effects on other traits, then the fixation of such mutations will select for compensatory mutations to mitigate the deleterious side effects, and evolution will proceed as a 'two steps forward, one step back' process. In systems where it is possible to identify the complete set of potentially causative mutations that are associated with an adaptive change in phenotype, key insights could be obtained by using reverse genetics experiments to measure the direct effects of individual mutations on the selected phenotype in conjunction with assessments of mutational pleiotropy in the same genetic background.

To investigate the nature of adaptive mutations and their pleiotropic effects, we used a protein engineering approach to characterize the molecular basis of hemoglobin (Hb) adaptation in the high-flying bar-headed goose (*Anser indicus*). This hypoxia-tolerant species is renowned for its trans-Himalayan migratory flights [10–12], and its elevated Hb-O_2 affinity is thought to make a key contribution to its capacity for powered flight at extreme elevations of 6000–9000 m [13–20]. At such elevations, an increased Hb-O_2 affinity helps safeguard arterial O_2 saturation, thereby compensating for the low O_2 tension of inspired air. This can help sustain O_2 delivery to metabolizing tissues because if environmental hypoxia is sufficiently severe, the benefit of increasing pulmonary O_2 loading typically outweighs the cost associated with a lower O_2 unloading pressure in the systemic circulation [21–24].

The Hb of birds and other jawed vertebrates is a heterotetramer consisting of two α-chain and two β-chain subunits. The Hb tetramer undergoes an oxygenation-linked transition in quaternary structure, whereby the two semi-rigid $\alpha_1\beta_1$ and $\alpha_2\beta_2$ dimers rotate around one another by 15˚ during the reversible switch between the deoxy (low-affinity [T]) conformation and the oxy (high-affinity [R]) conformation [25–28]. Oxygenation-linked shifts in the T↔R equilibrium govern the cooperativity of O_2-binding and are central to Hb's role in respiratory gas transport.

The major Hb isoform of the bar-headed goose has an appreciably higher O_2-affinity than that of the closely related greylag goose (*Anser anser*), a strictly lowland species [13,29]. The major Hbs of the two species differ at five amino acid sites: three in the α^A-chain subunit and two in the β^A-chain subunit [30,31]. Of these five amino acid differences, Perutz [32] predicted that the Pro→Ala replacement at α119 (αP119A) is primarily responsible for the adaptive increase in Hb-O_2 affinity in bar-headed goose. This site is located at an intersubunit ($\alpha_1\beta_1/\alpha_2\beta_2$) interface where the ancestral Pro α119 forms a van der Waals contact with Met β55 on the opposing subunit of the same αβ dimer. Perutz predicted that the single αP119A mutation

would eliminate this intradimer contact, thereby destabilizing the T-state and shifting the conformational equilibrium in favor of the high-affinity R-state. Jessen et al. [33] and Weber et al. [34] tested Perutz's hypothesis using a protein engineering approach based on site-directed mutagenesis of recombinant human Hb, and their experiments confirmed the predicted mechanism.

As a result of these experiments, bar-headed goose Hb is often held up as an example of a biochemical adaptation that is attributable to a single, large-effect substitution [35,36]. However, several key questions remain unanswered: Do the other substitutions also contribute to the change in Hb-O_2 affinity? If not, do they compensate for deleterious pleiotropic effects of the affinity-enhancing αP119A substitution? Given that the substitutions in question involve closely linked sites in the same gene, another possibility is that neutral mutations at the other sites simply hitchhiked to fixation along with the positively selected mutation. Since the other substitutions in bar-headed goose Hb have not been tested, we do not know whether αP119A accounts for all or most of the evolved change in O_2 affinity. Moreover, the original studies tested the effect of αP119A by introducing the goose-specific amino acid state into recombinant human Hb [33,34]. One potential problem with this type of 'horizontal' comparison–where residues are swapped between orthologous proteins of contemporary species–is that the focal mutation is introduced into a sequence context that is not evolutionarily relevant. If mutations have context-dependent effects, then introducing goose-specific substitutions into human Hb may not recapitulate the phenotypic effects of the mutations on the genetic background in which they actually occurred (i.e., in the ancestor of bar-headed goose). An alternative 'vertical' approach is to reconstruct and resurrect ancestral proteins to test the effects of historical mutations on the genetic background in which they actually occurred during evolution [37,38].

Here we revisit the functional evolution of bar-headed goose Hb, a classic text-book example of biochemical adaptation. We reconstructed the α^A- and β^A-chain Hb sequences of the most recent common ancestor of the bar-headed goose and its closest living relatives, all of which are lowland species in the genus *Anser*. After identifying the particular substitutions that are specific to bar-headed goose, we used a combinatorial approach to test the functional effects of each mutation in all possible multi-site combinations. To examine possible pleiotropic effects of causative mutations, we also measured several properties that potentially trade-off with Hb-O_2 affinity: susceptibility to spontaneous heme oxidation (autoxidation rate), allosteric regulatory capacity (the sensitivity of Hb-O_2 affinity to modulation by anionic effectors), and various secondary and tertiary structural properties. Measuring the direct and indirect effects of these mutations enabled us to address two fundamental questions about molecular adaptation: (*i*) Do each of the mutations contribute to the increased Hb-O_2 affinity? If so, what are their relative effects? And (*ii*) Do function-altering mutations have deleterious pleiotropic effects on other aspects of protein structure or function? If so, are these effects compensated by mutations at other sites?

Results and discussion

Direction of amino acid substitutions

Using globin sequences from bar-headed goose, greylag goose, and other waterfowl species in the subfamily Anserinae, we reconstructed the α- and β-chain sequences of the bar-headed goose/greylag goose ancestor, which we call 'AncAnser' because it represents the most recent common ancestor of all extant species in the genus *Anser* (Fig 1*A*). The principle of parsimony clearly indicates that all three of the α-chain substitutions that distinguish the Hbs of bar-headed goose and greylag goose occurred in the bar-headed goose lineage (Gα18S, Aα63V, and αP119A), whereas each of the two β-globin substitutions occurred in the greylag goose lineage (βT4S and βD125E)(Fig 1*A and* 1*B*).

Ancestral protein resurrection and functional testing

It is often implicitly assumed that the difference in Hb-O_2 affinity between bar-headed goose and greylag goose is attributable to a derived increase in Hb-O_2 affinity in the bar-headed

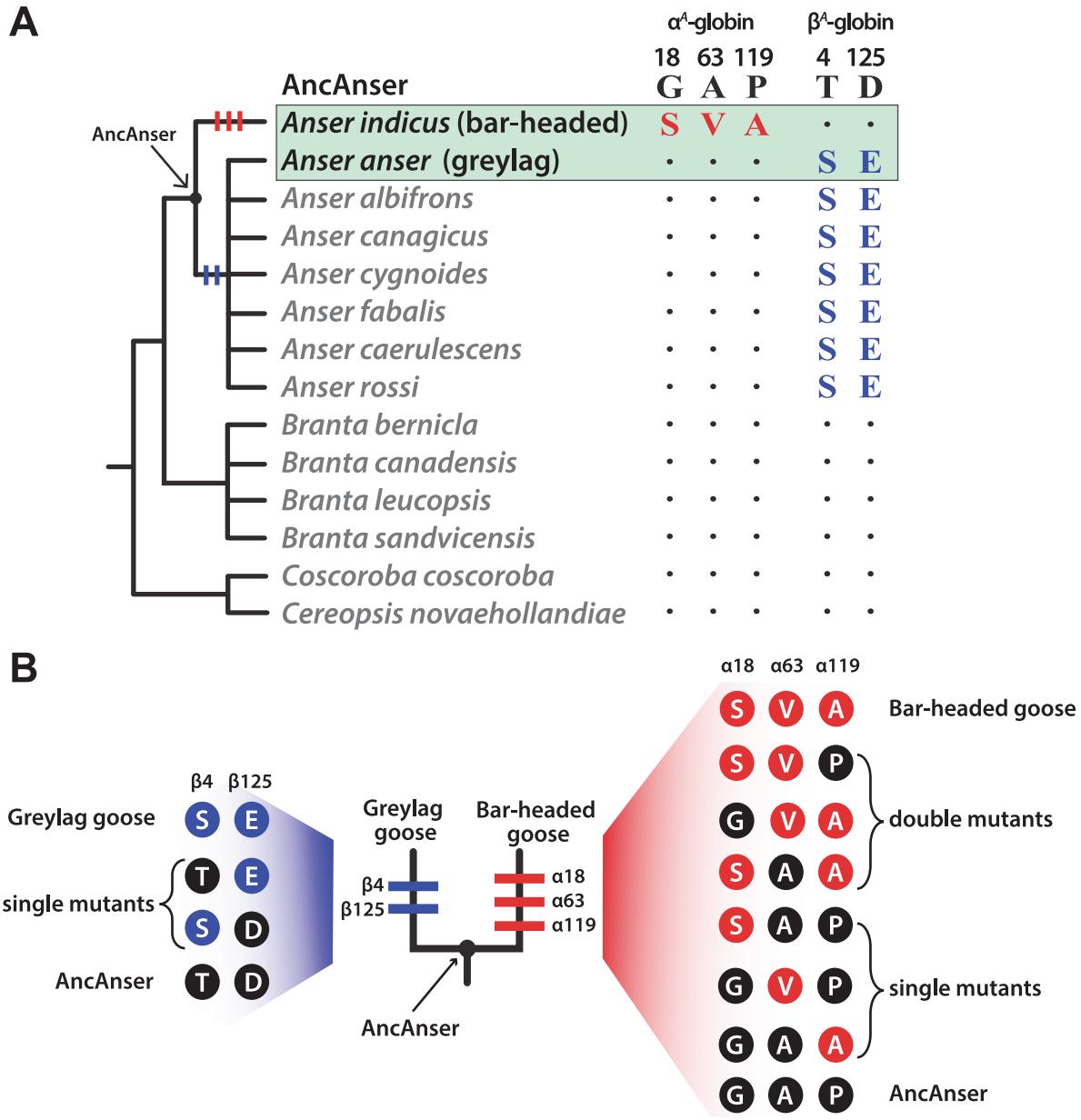

Fig 1. Inferred history of amino acid substitution at five sites that distinguish the major Hb isoforms of the bar-headed goose (*Anser indicus*) and greylag goose (*Anser anser*). (*A*) Amino acid states at the same sites are shown for 12 other waterfowl species in the subfamily Anserinae. Of the five amino acid substitutions that distinguish the Hbs of *A. indicus* and *A. anser*, parsimony indicates that three occurred on the branch leading to *A. indicus* (αG18S, αA63V, and αP119A) and two occurred on the branch subtending the clade of all *Anser* species other than *A. indicus* (βT4S and βD125E). 'AncAnser' represents the reconstructed sequence of the *A. indicus*/*A. anser* common ancestor, which is also the most recent common ancestor of all extant species in the genus *Anser*. (*B*) Triangulated comparisons involving rHbs of bar-headed goose, greylag goose, and their reconstructed ancestor (AncAnser) reveal the polarity of changes in character state. Differences in Hb function between bar-headed goose and AncAnser reflect the net effect of three substitutions (αG18S, αA63V, and αP119A) and differences between greylag goose and AncAnser reflect the net effect of two substitutions (βT4S and βD125E). All possible mutational intermediates connecting AncAnser with each of the two descendent species are shown to the side of each terminal branch (the sequential order of the substitutions is unknown, so the order in which they are shown on each terminal branch is arbitrary).

https://doi.org/10.1371/journal.pgen.1007331.g001

goose lineage [14,35,36,39]. In principle, however, the pattern could be at least partly attributable to a derived reduction in Hb-O_2 affinity in the greylag goose lineage, even if αP119A does account for the majority of the change in bar-headed goose. To resolve the polarity of character state change, we synthesized, purified, and functionally tested recombinant Hbs (rHbs) representing the wildtype Hb of bar-headed goose, the wildtype Hb of greylag goose, and the reconstructed Hb of their common ancestor, AncAnser. Functional differences between bar-headed goose and AncAnser rHbs reflect the net effect of three substitutions (αG18S, αA63V, and αP119A) and differences between greylag goose and AncAnser reflect the net effect of two substitutions (βT4S and βD125E; Fig 1*B*).

Since genetically based differences in Hb-O_2 affinity may be attributable to differences in intrinsic O_2-affinity and/or changes in sensitivity to allosteric effectors in the red blood cell, we measured O_2-equilibria of purified rHbs under four standardized treatments: (*i*) in the absence of allosteric effectors (stripped), (*ii*) in the presence of Cl^- ions (added as KCl), (*iii*) in the presence of inositol hexaphosphate (IHP, a chemical analog of the endogenously produced inositol pentaphosphate), and (*iv*) in the simultaneous presence of KCl and IHP. This latter treatment is most relevant to *in vivo* conditions in avian red blood cells. In each treatment, we measured P_{50}, the partial pressure of O_2 (PO_2) at which Hb is 50% saturated. To complement equilibrium measurements on the set of three rHbs and to gain further insight into functional mechanisms, we also performed stopped-flow kinetic experiments to estimate apparent O_2 dissociation rates under the same conditions.

The O_2-equilibrium measurements confirmed the results of previous studies [13,29] by demonstrating that the wildtype rHb of bar-headed goose has a higher intrinsic O_2-affinity than that of greylag goose (as revealed by the lower P_{50} for stripped Hb)(Fig 2*A*, Table 1). This difference persisted in the presence of Cl^- ions ($P_{50(KCl)}$), in the presence of IHP ($P_{50(IHP)}$), and in the simultaneous presence of both anions ($P_{50(KCl+IHP)}$)(Fig 2*A*, Table 1). All rHbs exhibited cooperative O_2-binding, as indicated by Hill coefficients (n_{50}'s) >2 in the presence of IHP. The difference in Hb-O_2 affinity between bar-headed goose and greylag goose is mainly attributable to differences in intrinsic affinity, as there were no appreciable differences in sensitivities to allosteric effectors (Table 1). This is consistent with a previous report that native Hbs of bar-headed goose and greylag goose have similarly high binding constants for inositol pentaphosphate [29]. Pairwise comparisons between each of the two modern-day species and their reconstructed ancestor (AncAnser) revealed that the elevated Hb-O_2 affinity of the bar-headed goose is a derived character state. O_2-equilibrium properties of greylag goose and AncAnser rHbs were generally very similar (Fig 2*A*). The triangulated comparison involving rHbs from the two contemporary species (bar-headed goose and greylag goose) and their reconstructed ancestor (AncAnser) revealed that the observed difference in Hb-O_2 affinity ($P_{50(KCl+IHP)}$) between bar-headed goose and greylag goose is mainly attributable to a derived increase in Hb-O_2 affinity in the bar-headed goose lineage, but it is also partly attributable to a derived reduction in Hb-O_2 affinity in the greylag goose lineage (Fig 2*A*). This demonstrates the value of ancestral protein resurrection for inferring the direction and magnitude of historical evolutionary changes in character state.

Kinetic measurements demonstrated that the increased O_2-affinity of bar-headed goose rHb is associated with a lower apparent rate of O_2 dissociation, k_{off} (Fig 2*B*) relative to the rHbs of both greylag goose and AncAnser.

Effects of individual substitutions in bar-headed goose Hb

In combination with the inferred history of sequence changes (Fig 1*A and* 1*B*), the comparison between the rHbs of bar-headed goose and AncAnser indicates that the derived increase in

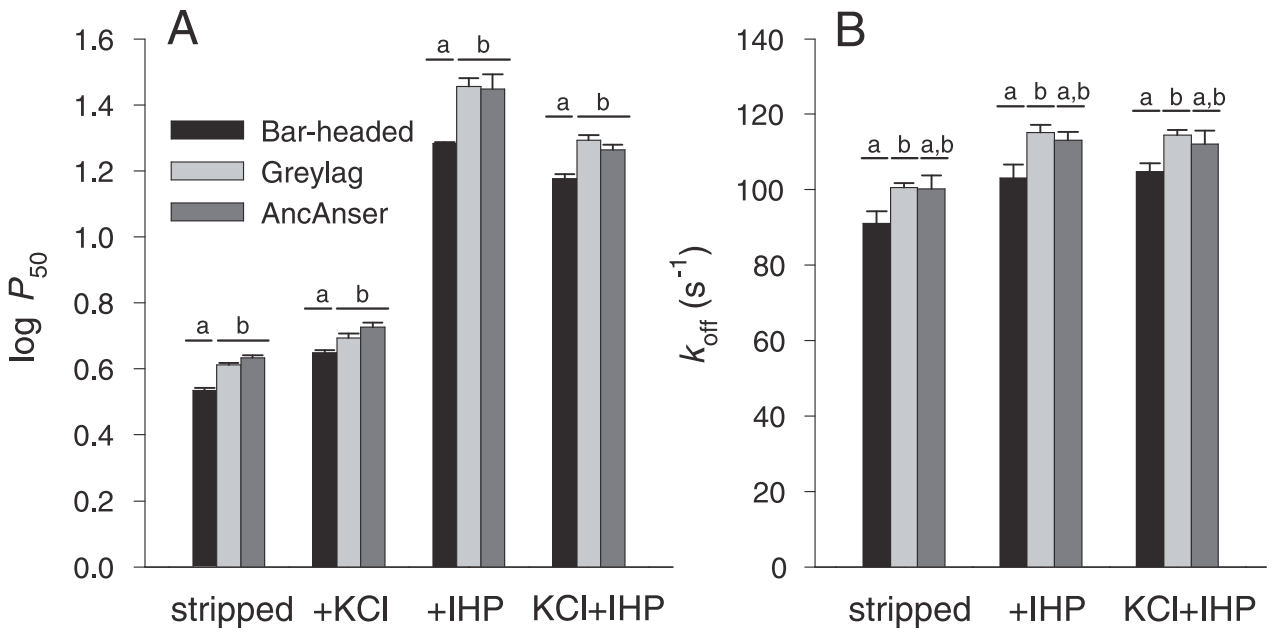

Fig 2. Bar-headed goose evolved an increased Hb-O_2 affinity relative to greylag goose and their reconstructed ancestor, AncAnser. Triangulated comparisons of purified rHbs involved diffusion-chamber measurements of O_2-equilibria (*A*) and stopped-flow measurements of O_2 dissociation kinetics (*B*). O_2-affinities (P_{50}, torr; ± 1 SEM) and dissociation rates (k_{off}, $M^{-1}s^{-1}$; ± 1 SEM) of purified rHbs were measured at pH 7.4, 37˚ C, in the absence (stripped) and presence of allosteric effectors ([Cl^-], 0.1 M; [Hepes], 0.1 M; IHP/Hb tetramer ratio = 2.0; [heme], 0.3 mM in equilibrium experiments; [Cl^-], 1.65 mM; [Hepes], 200 mM; IHP/Hb tetramer ratio = 2.0; [heme], 5 μM in kinetic experiments). Letters distinguish measured values that are significantly different ($P<0.05$).

https://doi.org/10.1371/journal.pgen.1007331.g002

Hb-O_2 affinity in bar-headed goose must be attributable to the independent or joint effects of the three substitutions at sites α18, α63, and α119. To measure the effects of each individual mutation in all possible multi-site combinations, we used site-directed mutagenesis to synthesize each of the six possible mutational intermediates that connect the ancestral and descendant genotypes (Fig 1*B*). In similar fashion, we synthesized each of the two possible mutational intermediates that connect AncAnser and the wildtype genotype of greylag goose (Fig 1*B*).

The analysis of the bar-headed goose mutations on the AncAnser background revealed that mutations at each of the three α-chain sites (αG18S, αA63V, and αP119A) produced significant increases in intrinsic Hb-O_2 affinity (indicated by reductions in $P_{50(stripped)}$)(Fig 3, Table 1). The Pα119A mutation had the largest effect on the ancestral background, producing an 18% reduction in $P_{50(stripped)}$ (increase in intrinsic Hb-O_2 affinity). On the same background, αG18S or αA63V produced 7% and 14% reductions in $P_{50(stripped)}$, respectively. In the set of six (= 3!) possible mutational pathways connecting the low-affinity AncAnser genotype (GAP) and the high-affinity bar-headed goose genotype (SVA), the αP119A mutation produced a significant increase in Hb-O_2 affinity on each of four possible backgrounds (corresponding to the first step in the pathway, two alternative second steps, and the third step; Fig 3). When tested on identical backgrounds, αP119A invariably produced a larger increase in intrinsic Hb-O_2 affinity than either αG18S or αA63V. Nonetheless, of the six possible forward pathways connecting GAP and SVA, αP119A had the largest effect in four pathways and αA63V had the largest effect in the remaining two. The two pathways in which αA63V had the largest effect were those in which it occurred as the first step. In fact, αG18S or αA63V only produced significant increases in Hb-O_2 affinity when they occurred as the first step. The effects of these two mutations were always smaller in magnitude when they occurred on backgrounds in which the derived Ala α119 was present. In addition to differences in average effect

Table 1. O_2 affinities (P_{50}, torr) and anion sensitivities ($\Delta\log P_{50}$) of rHbs representing bar-headed goose, greylag goose, their reconstructed ancestor (AncAnser), and all possible mutational intermediates connecting AncAnser with each of the two descendant species. O_2 equilibria were measured in 0.1 mM Hepes buffer at pH 7.4 (± 0.01) and 37˚C in the absence (stripped) and presence of Cl^- ions (0.1 M KCl]) and IHP (at two-fold molar excess over tetrameric Hb). Anion sensitivities are indexed by the difference in log-transformed values of P_{50} in the presence and absence of Cl^- ions (KCl) and IHP. The higher the $\Delta\log P_{50}$ value, the higher the sensitivity of Hb-O_2 affinity to the presence of a given anion or combination of anions. For the bar-headed goose mutants (all mutational intermediates between wild-type bar-headed goose and AncAnser), three-letter genotype codes denote amino acid states at α18, α63, and α119 (amino acid abbreviations underlined in bold = derived [non-ancestral]). At these same three sites, AncAnser is 'GAP' the wildtype genotype of bar-headed goose is 'SVA'. For the greylag goose mutants (all mutational intermediates between wildtype greylag goose and AncAnser), two-letter genotype codes denote amino acid states at β4 and β125. At these same two sites, AncAnser is 'TD' the wildtype genotype of greylag goose is 'SE'.

	P_{50} (± SE)	$\Delta\log P_{50}$		
rHb	**Stripped**	**+KCl**	**+IHP**	**KCl+IHP**
Bar-headed goose	3.42 ± 0.06	0.115	0.749	0.643
Greylag goose	4.10 ± 0.04	0.082	0.843	0.680
AncAnser	4.30 ± 0.06	0.092	0.815	0.630
Bar-headed goose mutants				
GA**A**	3.53 ± 0.08	0.111	0.745	0.693
G**V**P	3.68 ± 0.01	0.072	0.742	0.584
SAP	3.98 ± 0.03	0.098	0.653	0.523
G**VA**	3.52 ± 0.04	0.079	0.708	0.589
SA**A**	3.32 ± 0.05	0.156	0.870	0.742
SVP	3.88 ± 0.04	0.027	0.691	0.573
Greylag goose mutants				
SD	4.10 ± 0.05	0.052	0.729	0.601
T**E**	4.01 ± 0.04	0.104	0.774	0.549

https://doi.org/10.1371/journal.pgen.1007331.t001

size, αP119A also exhibited a higher degree of additivity across backgrounds than the other two mutations. For example, the affinity-enhancing effect of αP119A on the AncAnser background is mirrored by a similarly pronounced reduction in O_2-affinity when the mutation is reverted on the wildtype bar-headed goose background (αA119P). By contrast, forward and reverse mutations at α18 and α63 do not show the same symmetry of effect (S1 Fig).

Structural mechanisms underlying the evolved increase in Hb-O_2 affinity in bar-headed goose

Comparison of crystal structures for human and bar-headed goose Hbs [40] revealed that each of the three bar-headed goose α-chain substitutions have structurally localized effects. In the major bar-headed goose Hb isoform, Ser α18 and Ala α119 are located at the edges of the $\alpha_1\beta_1$ intradimer interface. As noted by Jessen et al. [33], the αP119A mutation has very little effect on the main-chain formation and appears to exert its functional effect via the elimination of side chain contacts and increased backbone flexibility. With regard to the αA63V mutation, the introduction of the valine side chain causes minor steric clashes with Gly 25 and Gly 59 of the same subunit (Fig 4). This interaction may alter O_2-affinity by impinging on the neighboring His α58, the 'distal histidine' that stabilizes the α-heme Fe-O_2 bond [41–46].

Effects of individual substitutions in greylag goose Hb

Given that the AncAnser and greylag goose rHbs exhibit similar equilibrium and kinetic O_2-binding properties (Fig 2), the two greylag goose substitutions (βT4S and βD125E) do not

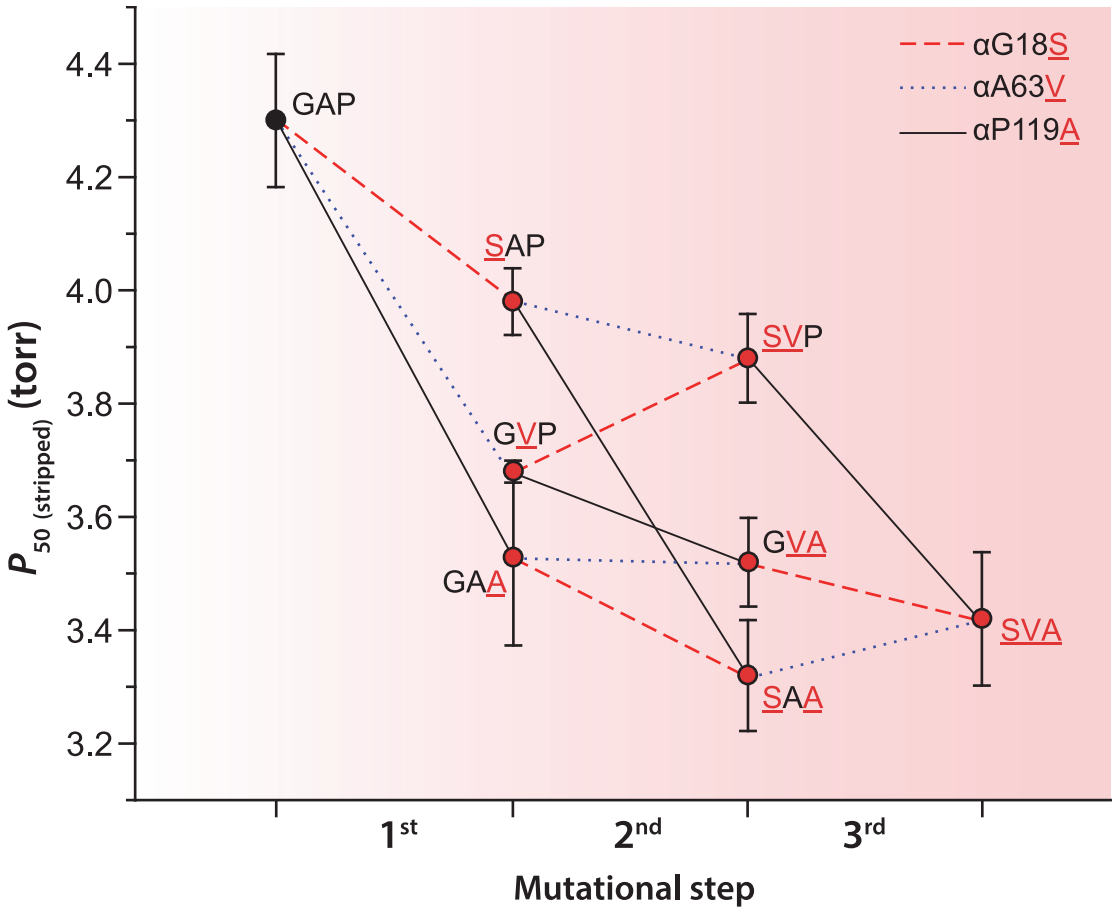

Fig 3. Trajectories of change in intrinsic Hb-O_2 affinity (indexed by P_{50}, torr) in each of six possible forward pathways that connect the ancestral 'AncAnser' genotype (GAP) and the wildtype genotype of bar-headed goose (SVA). Derived amino acid states are indicated by red lettering. Error bars denote 95% confidence intervals.

https://doi.org/10.1371/journal.pgen.1007331.g003

produce an appreciable net change in combination. Interestingly, however, each mutation by itself produces a slightly reduced sensitivity to IHP (Table 1), such that values of $P_{50(IHP)}$ and $P_{50(KCl+IHP)}$ for the single-mutant intermediates were lower than those for AncAnser and the wildtype genotype of greylag goose.

Mutational pleiotropy

Since amino acid mutations often affect multiple aspects of protein biochemistry [47–50], it is of interest to test whether adaptive mutations that improve one aspect of protein function simultaneously compromise other properties. Amino acid mutations that alter the oxygenation properties of Hb often have pleiotropic effects on allosteric regulatory capacity, structural stability, and susceptibility to heme loss and/or heme oxidation [51–58]. Accordingly, we tested whether mutational changes in intrinsic O_2-affinity are associated with potentially deleterious changes in other structural and functional properties.

Analysis of the full set of bar-headed goose and greylag goose rHb mutants revealed modest variability in autoxidation rate (S2*A* Fig, Table 2). This property is physiologically relevant because oxidation of the ferrous (Fe^{2+}) heme iron to the ferric state (Fe^{3+}) releases superoxide (O_2^-) or perhydroxy (HO_2•) radical, and prevents reversible Fe-O_2 binding, rendering Hb

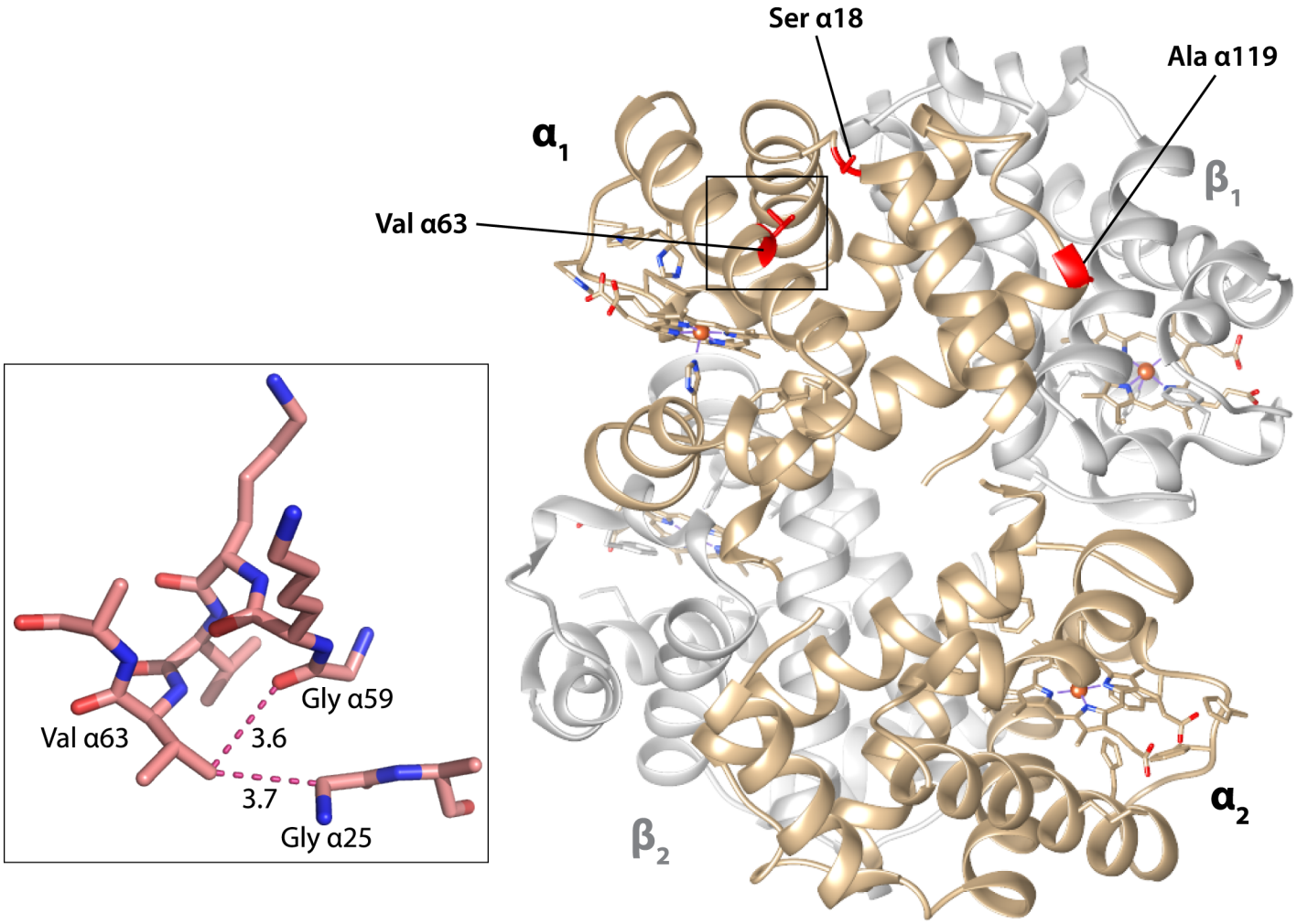

Fig 4. Structural model showing bar-headed goose Hb in the deoxy state (PDB1hv4), along with locations of each of the three amino substitutions that occurred in the bar-headed goose lineage after divergence from the common ancestor of other *Anser* species. The inset graphic shows the environment of the Val α63 residue. When valine replaces the ancestral alanine at this position, the larger volume of the side-chain causes minor steric clashes with two neighboring glycine residues, Gly α25 and Gly α59. The distances between non-hydrogen atoms (depicted by dotted lines) are given in Å.

https://doi.org/10.1371/journal.pgen.1007331.g004

inoperative as an O_2-transport molecule. Although mutational changes in intrinsic O_2 affinity ($\Delta\log P_{50(\text{stripped})}$) were not significantly correlated with changes in autoxidation rate in the full dataset (r = -0.311), analysis of the bar-headed goose rHb mutants revealed a striking pairwise interaction between mutations at α18 and α63 (residues which are located within 7 Å of one another). The αA63V mutation produced a significant >2-fold increase in the autoxidation rate on backgrounds in which the ancestral Gly is present at α18 (Fig 5, Table 2). The adjacent Val α62 is highly conserved because it plays a critical role in restricting solvent access to the distal heme pocket, thereby preventing water-catalyzed rupture of the Fe-O_2 bond to release a superoxide ion [58–61]. An increase in side chain volume at α63 may compromise this gating function, resulting in an increased susceptibility to heme oxidation. The increased autoxidation rate caused by αA63V is fully compensated by αG18S (Fig 5), a highly unusual amino acid replacement because glycine is the only amino acid at this site (the C-terminal end of the A helix) that permits the main chain to adopt the typical Ramachandran angles (S3 Fig).

Table 2. Autoxidation rates of rHbs representing bar-headed goose, greylag goose, their reconstructed ancestor (AncAnser), and all possible mutational intermediates connecting AncAnser with each of the two descendant species. For the bar-headed goose mutants (all mutational intermediates between wildtype bar-headed goose and AncAnser), three-letter genotype codes denote amino acid states at α18, α63, and α119 (amino acid abbreviations underlined in bold = derived [non-ancestral]). At these same three sites, AncAnser is 'GAP' the wildtype genotype of bar-headed goose is 'SVA'. For the greylag goose mutants (all mutational intermediates between wildtype greylag goose and AncAnser), two-letter genotype codes denote amino acid states at β4 and β125. At these same two sites, AncAnser is 'TD' the wildtype genotype of greylag goose is 'SE'.

rHb	Autoxidation rate, h^{-1} (± SEM)
Bar-headed goose	0.109 ± 0.017
Greylag goose	0.112 ± 0.019
AncAnser	0.170 ± 0.014
Bar-headed goose mutants	
GA**A**	0.164 ± 0.026
G**V**P	0.399 ± 0.067
SAP	0.149 ± 0.011
G**VA**	0.424 ± 0.036
SAA	0.154 ± 0.013
SVP	0.159 ± 0.009
Greylag goose mutants	
SD	0.132 ± 0.014
T**E**	0.156 ± 0.019

https://doi.org/10.1371/journal.pgen.1007331.t002

Introduction of the serine side chain at α18 in bar-headed goose Hb forces this residue to undergo a peptide flip relative to human Hb, so the carbonyl oxygen points in the opposite direction. This unusual replacement at α18 may be required to accommodate the bulkier Val side chain at α63, thereby alleviating conformational stress. Site-directed mutagenesis experiments on mutant Hbs and myoglobins have documented a positive, linear correlation between $\log(P_{50})$ and $\log(k_{auto})$ [58–61]. The αG18S and αA63V mutations are therefore unusual

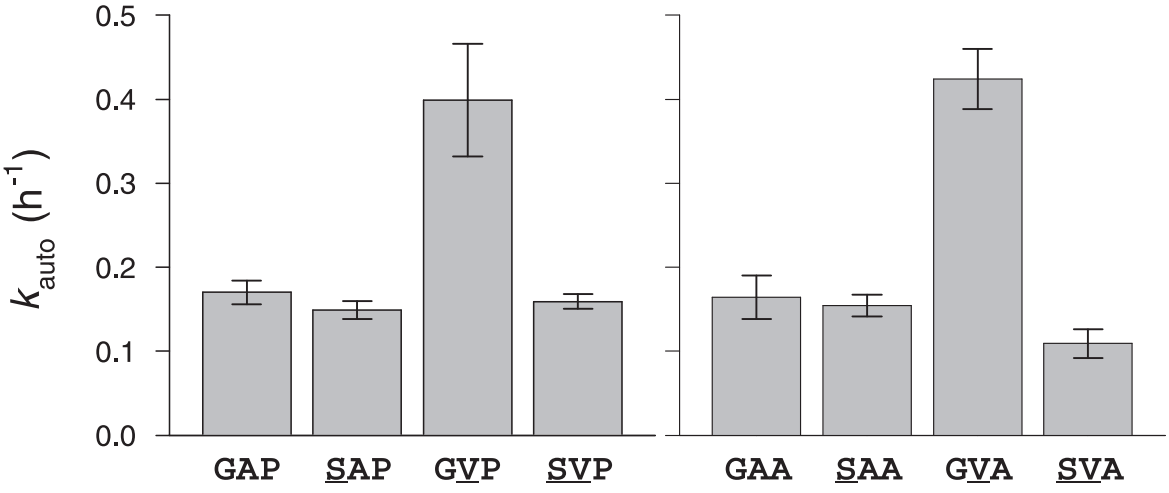

Fig 5. Compensatory interaction between spatially proximal α-chain residues in bar-headed goose Hb. The mutation Aα63V produces a >2-fold increase in autoxidation rate (k_{auto}; ± 1 SEM) on genetic backgrounds with the ancestral Gly at residue position α18. This effect is fully compensated by Gα18S, as indicated by two double-mutant cycles (*A* and *B*) in which mutations at both sites are tested individually and in pairwise combination.

https://doi.org/10.1371/journal.pgen.1007331.g005

because reductions in Hb-O_2 affinity are not invariably coupled with increases in autoxidation rate.

Aside from the compensatory interaction between mutations at α18 and α63, we observed no evidence for trade-offs between O_2-affinity and any of the other measured functional or structural properties. There were no significant correlations between Δlog $P_{50(stripped)}$ and changes in allosteric regulatory capacity (Table 1), as measured by sensitivity to Cl^- (r = -0.534), IHP (r = -0.137), or both anions in combination (r = -0.300). The goose rHbs revealed no appreciable variation in α-helical secondary structure as measured by circular dichroism spectroscopy (S2*B* Fig, S1 Table) and there were no significant correlations between Δlog $P_{50(stripped)}$ and changes in secondary structure over the physiological range (pH 6.5, r = -0.357; pH 7.5, r = -0.052). Likewise, the rHbs exhibited very little variation in the stability of tertiary structure as measured by UV-visible spectroscopy (S2*C* Fig, S2 Table) and there were no significant correlations between Δlog $P_{50(stripped)}$ and changes in stability over the physiological range (pH 6.5, r = -0.511; pH 7.5, r = -0.338). In summary, we found no evidence for pleiotropic trade-offs between intrinsic O_2-affinity and any measured properties of Hb structure or function other than autoxidation rate.

Conclusions

We now return to the two questions we posed at the outset:

(1) Do each of the bar-headed goose substitutions contribute to the increased Hb-O_2 affinity?

It depends on the order in which the substitutions occur. Our experiments demonstrated that the αP119A mutation always produced a significant increase in intrinsic Hb-O_2 affinity regardless of the background in which it occurred. As documented previously [33,34], the αP119A mutation also produces a significant affinity-enhancing effect on the far more divergent background of human Hb (which differs from bar-headed goose Hb at 89 of 267 amino acid sites in each αβ half-molecule [33% divergence in protein sequence]). By contrast, αG18S or αA63V only produced significant affinity-enhancing effects when they occurred as the first step in the pathway (on the AncAnser background). If it was advantageous for the ancestor of today's bar-headed geese to have an increased Hb-O_2 affinity, our experiments suggest that any of the three α-chain mutations alone would have conferred a beneficial effect, but only αP119A would have produced the same effect after the other two had already fixed. This illustrates an important point about distributions of mutational effect sizes in adaptive walks: in the presence of epistasis, relative effect sizes may be highly dependent on the sequential order in which the substitutions occur.

(2) Do function-altering mutations have deleterious pleiotropic effects on other aspects of protein structure or function?

On the AncAnser background, the affinity-enhancing mutation, αA63V, produces a pronounced increase in the autoxidation rate. This is consistent with the fact that engineered Hb and myoglobin mutants with altered affinities often exhibit increased autoxidation rates [54,56,58,62]. In the case of bar-headed goose Hb, the increased autoxidation rate caused by αA63V is completely compensated by a polarity-changing mutation at a spatially proximal site, αG18S. This compensatory interaction suggests that the αG18S mutation may have been fixed by selection not because it produced a beneficial main effect on Hb-O_2 affinity, but because it mitigated the deleterious pleiotropic effects of the affinity-altering αA63V mutation. Alternatively, if αG18S preceded αA63V during the evolution of bar-headed goose Hb, then the (conditionally) deleterious side effects of αA63V would not have been manifest.

Our experiments revealed no evidence to suggest that the affinity-altering αP119A mutation perturbed other structural and functional properties of Hb. Data on natural and

engineered human Hb mutants have provided important insights into structure-function relationships and the nature of trade-offs between different functional properties [52,54,56–58,63]. An important question concerns the extent to which function-altering spontaneous mutations are generally representative of those that eventually fix and contribute to divergence in protein function between species. There are good reasons to expect that the spectrum of pleiotropic effects among spontaneous mutations or low-frequency variants may be different from the spectrum of effects among evolutionary substitutions (mutations that passed through the filter of purifying selection and eventually increased to a frequency of 1.0) [64]. The affinity-altering mutations that are most likely to fix (whether due to drift or positive selection) may be those that have minimal pleiotropic effects and therefore do not require compensatory mutations at other sites.

Materials and methods

Sequence data

We took sequence data for the α^A- and β^A-globin genes of all waterfowl species from published sources [30,31].

Vector construction and site-directed mutagenesis

After optimizing nucleotide sequences of AncAnser α^A- and β^A-globin genes in accordance with *E. coli* codon preferences, we synthesized the α^A-β^A-globin cassette (Eurofins MWG Operon). We cloned the globin cassette into a custom pGM vector system [65,66], as described previously [67–74], and we then used site-directed mutagenesis to derive globin sequences of greylag goose, bar-headed goose, and each of the mutational intermediates connecting these wildtype sequences with AncAnser. We conducted the codon mutagenesis using the QuikChange II XL Site-Directed Mutagenesis kit (Agilent Technologies) and we verified all codon changes by DNA sequencing.

Expression and purification of recombinant Hbs

We carried out recombinant Hb (rHb) expression in the *E. coli* JM109 (DE3) strain as described previously [66]. To ensure the complete cleavage of N-terminal methionines from the nascent globin chains, we over-expressed methionine aminopeptidase (MAP) by co-transforming a plasmid (pCO-MAP) along with a kanamycin resistance gene (48). We then co-transformed the pGM and pCO-MAP plasmids and subjected them to dual selection in an LB agar plate containing ampicillin and kanamycin. We carried out the over expression of each rHb mutant in 1.5 L of TB medium.

We grew bacterial cells at 37˚C in an orbital shaker at 200 rpm until absorbance values reached 0.6 to 0.8 at 600 nm. We then induced the bacterial cultures with 0.2 mM IPTG and supplemented them with hemin (50 μg/ml) and glucose (20 g/L). The bacterial culture conditions and the protocol for preparing cell lysates were described previously [66]. We resuspended bacterial cells in lysis buffer (50 mM Tris, 1 mM EDTA, 0.5 mM DTT, pH 7.0) with lysozyme (1 mg/g wet cells) and incubated them in an ice bath for 30 min. Following sonication of the cells, we added 0.5–1.0% polyethyleneimine solution, and we then centrifuged the crude lysate at 13,000 rpm for 45 min at 4˚C.

We purified the rHbs by means of two-step ion-exchange chromatography. Using high-performance liquid chromatography (Äkta start, GE Healthcare), we passed the samples through a cation exchange-column (SP-Sepharose) followed by passage through an anion-exchange column (Q-Sepharose). We subjected the clarified supernatant to overnight dialysis in Hepes buffer (20 mM Hepes with 0.5mM EDTA, 1 mM DTT, 0.5mM IHP, pH 7.0) at 4˚C. We used

prepackaged SP-Sepharose columns (HiTrap SPHP, 5 mL, 17–516101; GE Healthcare) equilibrated with Hepes buffer (20 mM Hepes with 0.5mM EDTA, 1 mM DTT, 0.5mM IHP pH 7.0). After passing the samples through the column, we eluted the rHb solutions against a linear gradient of 0–1.0 M NaCl. After desalting the eluted samples, we performed an overnight dialysis against Tris buffer (20 mM Tris, 0.5mM EDTA, 1 mM DTT, pH 8.4) at 4˚C. We then passed the dialyzed samples through a pre-equilibrated Q-Sepharose column (HiTrap QHP, 1 mL, 17-5158-01; GE Healthcare) with Tris buffer (20 mM Tris, 0.5mM EDTA, 1 mM DTT, pH 8.4). We eluted the rHb samples with a linear gradient of 0–1.0 M NaCl. We then concentrated the samples and desalted them by means of overnight dialysis against 10 mM Hepes buffer (pH 7.4). We then stored the purified samples at -80˚ C prior to the measurement of O_2-equilibria and O_2 dissociation kinetics. We analyzed the purified rHb samples by means of sodium dodecyl sulphate (SDS) polyacrylamide gel electrophoresis and isoelectric focusing. After preparing rHb samples as oxyHb, deoxyHb, and carbonmonoxy derivatives, we measured absorbance at 450–600 nm to confirm the expected absorbance maxima.

Measurement of Hb-O_2 equilibria

Using purified rHb solutions (0.3 mM heme), we measured O_2-equilibrium curves at 37˚C in 0.1 M Hepes buffer (pH 7.4) in the absence ('stripped') and presence of 0.1 M KCl and IHP (at two-fold molar excess over tetrameric Hb), and in the simultaneous presence of KCl and IHP. We measured O_2-equilibria of 5 μl thin-film samples in a modified diffusion chamber where absorption at 436 nm was monitored during stepwise changes in the equilibration of N_2/O_2 gas mixtures generated by precision Wösthoff mixing pumps [75–77]. We estimated values of P_{50} and n_{50} (Hill's cooperativity coefficient) by fitting the Hill equation $Y = PO_2{}^n/(P_{50}{}^n + PO_2{}^n)$ to the experimental O_2 saturation data by means of nonlinear regression (Y = fractional O_2 saturation; n, cooperativity coefficient). Standard errors of the mean P_{50} were based on triplicate measurements of independently purified rHbs, and the nonlinear fitting of each curve was based on 5–8 equilibration steps. Free Cl^- concentrations were measured with a model 926S Mark II chloride analyzer (Sherwood Scientific Ltd, Cambridge, UK).

Measurement of Hb-O_2 dissociation kinetics

We determined apparent O_2 dissociation constants (k_{off}) of purified oxy rHbs at 37˚C using an OLIS RSM 1000 UV/Vis rapid-scanning stopped flow spectrophotometer (OLIS, Bogart, CA) equipped with an OLIS data collection software. Briefly, rHb (10 μM heme) in 200 mM Hepes, pH 7.4, was mixed 1:1 with N_2-equilibrated 200 mM Hepes, pH 7.4, containing 40 mM freshly dissolved sodium dithionite [78]. We monitored absorbance at 431 nm as a function of time. All traces exhibited the best fit to a monoexponential function ($r^2 > 0.99$).

Measurement of autoxidation rates

To estimate autoxidation rates, we treated purified rHb samples with potassium ferricyanide ($K_3[Fe(CN)_6]$), and we then reduced rHbs to the ferrous (Fe^{2+}) state by treating the samples with sodium dithionite ($Na_2S_2O_4$). We removed the dithionite by means of chromatography (Sephadex G-50). For each rate measurement, we used 200 μl of 20 μM oxyHb in 100 mM potassium phosphate buffer, pH 7.0, containing 1 mM EDTA and 3 mM catalase and superoxide dismutase per mole oxyHb. To measure the spontaneous conversion of ferrous (Fe^{2+}) oxyHb to ferric (Fe^{3+}) metHb we recorded the absorbance spectrum at regular intervals over a 90 h period. We collected spectra between 400nm and 700nm using a BioTek Synergy2 multimode microplate reader (BioTek Instruments). We estimated autoxidation rates by plotting the A_{541}/A_{630} ratio (ratio of absorbances at 540nm and 630nm) vs time, using IGOR Pro 6.37

software (Wavemetrics). We used the exponential offset formula in IGOR to calculate the 50% absorbance per half-life (i.e., 0.5AU/half-life). Standard errors of the mean autoxidation rate were based on triplicate measurements of independently purified rHbs.

Measurements of secondary and tertiary structural properties

We assessed the pH-dependent stability of the rHbs by means of UV-visible spectroscopy. We prepared 20 mM filtered buffers spanning the pH range 2.0–11.0. We prepared 20 mM glycine-HCl for pH 2.0–3.5; 20 mM acetate for pH 4.0–5.5; 20 mM phosphate for pH 6.0–8.0; 20 mM glycine-NaOH for pH 8.5–10.0; 20 mM carbonate-NaOH for pH 10.5 and phosphate-NaOH for pH 11.0. We diluted the purified rHb samples in the pH-specific buffers to achieve uniform protein concentrations of 0.15 mg/ml. We incubated the samples for 3–4 h at 25˚C prior to spectroscopic measurements, and maintained this same temperature during the course of the experiments. We measured absorbance in the range 260–700 nm using a Cary Varian Bio100 UV-Vis spectrophotometer (Varian) with Quartz cuvettes, and used IGOR Pro 6.37 (WaveMetrics) to process the raw spectra. For the same set of rHbs, we tested for changes in secondary structure of the globin chains by measuring circular dichroism spectra on a JASCO J-815 spectropolarimeter using a quartz cell with a path length of 1 mm. We assessed changes in secondary structure by measuring molar ellipticity in the far UV region between 190 and 260 nm in three consecutive spectral scans per sample.

Structural modeling

We modelled structures of goose Hbs and the various mutational intermediates using the program COOT [79], based on the crystal structures of bar-headed goose Hb (PDB models 1hv4 and 1c40)[40,80], greylag goose Hb (PDB 1faw)[81], and human deoxyHb (PDB 2dn2).

Supporting information

S1 Fig. The αP119A mutation has consistent effects on Hb-O_2 affinity on different genetic backgrounds. The affinity-enhancing effect of αP119A on the AncAnser background is mirrored by a similarly pronounced affinity-reducing effect when the mutation is reverted on the wildtype bar-headed goose background (αA119P). By contrast, forward and reverse mutations at α18 and α63 do not show the same symmetry of effect, indicating that their effects are conditional on the amino acid state at one or both of the other two sites.
(PDF)

S2 Fig. Variation among goose rHb mutants in functional and structural properties that potentially trade-off with intrinsic O_2 affinity. Variation in (*A*) autoxidation rate (rate at which ferrous heme [Fe^{2+}] spontaneously oxidizes to the ferric state [Fe^{3+}]), (*B*) secondary structure content, as assessed by means of circular dichroism spectra (with ellipticity measured in millidegrees [mdeg], 222 nm) at pH 7.0 and 7.5 (physiological range), and (*C*) stability of tertiary structure and holoprotein, as assessed by means of UV-visible spectroscopy (absorbance measured at 412 nm) at pH 7.0 and 7.5 (physiological range). For stability measurements over the full pH range, see S1 and S2 Tables.
(PDF)

S3 Fig. Ramachandran plot of deoxyHb from bar-headed goose (PDB 1hv4). Glycine residues are denoted by triangles, other residues by squares. One residue, α18-Ser, is conspicuous by its unusual backbone angles, and is shown as a green square. This position in the Ramachandran plot is highly unusual for any residue other than glycine. The turn in the backbone between the A and B helices can only be accommodated by a glycine, since the lack of a side-

chain avoids the strong steric clash that would develop between a C_β atom and the nitrogen atom of residue 19. The serine at α18 is therefore forced to flip the peptide conformation, such that its carbonyl group points in the opposite direction relative to that of Gly 18.
(PDF)

S1 Table. Effect of pH on the stability of tertiary structure, as measured by UV-visible spectroscopy. Measurements of absorbance maxima at 412 nm are shown for rHbs representing wildtype genotypes of bar-headed goose (BHG), greylag goose (GG), their reconstructed ancestor (AncAnser), and all possible mutational intermediates connecting AncAnser with each of the two descendant species. For the bar-headed goose mutants (all mutational intermediates between wildtype bar-headed goose and AncAnser), three-letter genotype codes denote amino acid states at α18, α63, and α119 (amino acid abbreviations in black lettering = ancestral, red lettering = derived). At these same three sites, AncAnser is 'GAP' the wildtype genotype of bar-headed goose is 'SVA'. For the greylag goose mutants (all mutational intermediates between wildtype greylag goose and AncAnser), two-letter genotype codes denote amino acid states at β4 and β125 (amino acid abbreviations in black lettering = ancestral, blue lettering = derived). At these same two sites, AncAnser is 'TD' the wildtype genotype of greylag goose is 'SE'.
(DOCX)

S2 Table. Stability of α-helical secondary structure as a function of pH, measured by circular dichroism spectroscopy. Measurements of molar ellipticity are shown for rHbs representing wildtype genotypes of bar-headed goose (BHG), greylag goose (GG), their reconstructed ancestor (AncAnser), and all possible mutational intermediates connecting AncAnser with each of the two descendant species. For the bar-headed goose mutants (all mutational intermediates between wildtype bar-headed goose and AncAnser), three-letter genotype codes denote amino acid states at α18, α63, and α119 (amino acid abbreviations in black lettering = ancestral, red lettering = derived). At these same three sites, AncAnser is 'GAP' the wildtype genotype of bar-headed goose is 'SVA'. For the greylag goose mutants (all mutational intermediates between wildtype greylag goose and AncAnser), two-letter genotype codes denote amino acid states at β4 and β125 (amino acid abbreviations in black lettering = ancestral, blue lettering = derived). At these same two sites, AncAnser is 'TD' the wildtype genotype of greylag goose is 'SE'.
(DOCX)

Acknowledgments

We thank E. E. Petersen for skilled assistance, H. Moriyama for sharing equipment, K. G. McCracken for helpful discussion, and several anonymous reviewers for constructive critiques.

Author Contributions

Conceptualization: Chandrasekhar Natarajan, Angela Fago, Jay F. Storz.

Formal analysis: Chandrasekhar Natarajan, Jeremy R. H. Tame, Angela Fago, Jay F. Storz.

Funding acquisition: Jay F. Storz.

Investigation: Chandrasekhar Natarajan, Agnieszka Jendroszek, Amit Kumar, Jeremy R. H. Tame, Angela Fago, Jay F. Storz.

Project administration: Jay F. Storz.

Supervision: Roy E. Weber, Angela Fago, Jay F. Storz.

Writing – original draft: Jay F. Storz.

Writing – review & editing: Chandrasekhar Natarajan, Roy E. Weber, Jeremy R. H. Tame, Angela Fago.

References

1. Burch CL, Chao L (1999) Evolution by small steps and rugged landscapes in the RNA virus phi 6. Genetics 151: 921–927. PMID: 10049911
2. Moore FBG, Rozen DE, Lenski RE (2000) Pervasive compensatory adaptation in *Escherichia coli*. Proceedings of the Royal Society B-Biological Sciences 267: 515–522.
3. Stern DL (2000) Evolutionary developmental biology and the problem of variation. Evolution 54: 1079–1091. PMID: 11005278
4. Otto SP (2004) Two steps forward, one step back: the pleiotropic effects of favoured alleles. Proceedings of the Royal Society B-Biological Sciences 271: 705–714.
5. Ostrowski EA, Rozen DE, Lenski RE (2005) Pleiotropic effects of beneficial mutations in *Escherichia coli*. Evolution 59: 2343–2352. PMID: 16396175
6. Poon AFY, Chao L (2006) Functional origins of fitness effect-sizes of compensatory mutations in the DNA bacteriophage phi X174. Evolution 60: 2032–2043. PMID: 17133860
7. Cooper TF, Ostrowski EA, Travisano M (2007) A negative relationship between mutation pleiotropy and fitness effect in yeast. Evolution 61: 1495–1499. https://doi.org/10.1111/j.1558-5646.2007.00109.x PMID: 17542856
8. Qian WF, Ma D, Xiao C, Wang Z, Zhang JZ (2012) The genomic landscape and evolutionary resolution of antagonistic pleiotropy in yeast. Cell Reports 2: 1399–1410. https://doi.org/10.1016/j.celrep.2012.09.017 PMID: 23103169
9. Szamecz B, Boross G, Kalapis D, Kovacs K, Fekete G, et al. (2014) The genomic landscape of compensatory evolution. PloS Biology 12, e1001935. https://doi.org/10.1371/journal.pbio.1001935 PMID: 25157590
10. Hawkes LA, Balachandran S, Batbayar N, Butler PJ, Frappell PB, et al. (2011) The trans-Himalayan flights of bar-headed geese (*Anser indicus*). Proceedings of the National Academy of Sciences of the United States of America 108: 9516–9519. https://doi.org/10.1073/pnas.1017295108 PMID: 21628594
11. Hawkes LA, Balachandran S, Batbayar N, Butler PJ, Chua B, et al. (2013) The paradox of extreme high-altitude migration in bar-headed geese *Anser indicus*. Proceedings of the Royal Society B-Biological Sciences 280.
12. Bishop CM, Spivey RJ, Hawkes LA, Batbayar N, Chua B, et al. (2015) The roller coaster flight strategy of bar-headed geese conserves energy during Himalayan migrations. Science 347: 250–254. https://doi.org/10.1126/science.1258732 PMID: 25593180
13. Petschow D, Wurdinger I, Baumann R, Duhm J, Braunitzer G, et al. (1977) Causes of high blood O_2 affinity of animals living at high-altitude. Journal of Applied Physiology 42: 139–143. https://doi.org/10.1152/jappl.1977.42.2.139 PMID: 14096
14. Black CP, Tenney SM (1980) Oxygen-transport during progressive hypoxia in high-altitude and sea-level waterfowl. Respiration Physiology 39: 217–239. PMID: 7375742
15. Faraci FM (1986) Circulation during hypoxia in birds. Comparative Biochemistry and Physiology A-Physiology 85: 613–620.
16. Scott GR, Milsom WK (2006) Flying high: A theoretical analysis of the factors limiting exercise performance in birds at altitude. Respiratory Physiology and Neurobiology 154: 284–301. https://doi.org/10.1016/j.resp.2006.02.012 PMID: 16563881
17. Scott GR, Milsom WK (2007) Control of breathing and adaptation to high altitude in the bar-headed goose. American Journal of Physiology-Regulatory Integrative and Comparative Physiology 293: R379–R391.
18. Scott GR (2011) Elevated performance: the unique physiology of birds that fly at high altitudes. Journal of Experimental Biology 214: 2455–2462. https://doi.org/10.1242/jeb.052548 PMID: 21753038
19. Meir JU, Milsom WK (2013) High thermal sensitivity of blood enhances oxygen delivery in the high-flying bar-headed goose. Journal of Experimental Biology 216: 2172–2175. https://doi.org/10.1242/jeb.085282 PMID: 23470665

20. Scott GR, Hawkes LA, Frappell PB, Butler PJ, Bishop CM, et al. (2015) How bar-headed geese fly over the Himalayas. Physiology 30: 107–115. https://doi.org/10.1152/physiol.00050.2014 PMID: 25729056
21. Bencowitz HZ, Wagner PD, West JB (1982) Effect of change in P_{50} on exercise tolerance at high-altitude—a theoretical study. Journal of Applied Physiology 53: 1487–1495. https://doi.org/10.1152/jappl.1982.53.6.1487 PMID: 7153147
22. Willford DC, Hill EP, Moores WY (1982) Theoretical analysis of optimal P_{50}. Journal of Applied Physiology 52: 1043–1048. https://doi.org/10.1152/jappl.1982.52.4.1043 PMID: 7085405
23. Storz JF, Scott GR, Cheviron ZA (2010) Phenotypic plasticity and genetic adaptation to high-altitude hypoxia in vertebrates. Journal of Experimental Biology 213: 4125–4136. https://doi.org/10.1242/jeb.048181 PMID: 21112992
24. Storz JF (2016) Hemoglobin-oxygen affinity in high-altitude vertebrates: Is there evidence for an adaptive trend? Journal of Experimental Biology 219: 3190–3203. https://doi.org/10.1242/jeb.127134 PMID: 27802149
25. Perutz MF (1972) Nature of heme-heme interaction. Nature 237: 495–499. PMID: 12635193
26. Baldwin J, Chothia C (1979) Haemoglobin: the structural changes related to ligand binding and its allosteric mechanism. Journal of Molecular Biology 129: 175–220. PMID: 39173
27. Lukin JA, Ho C (2004) The structure-function relationship of hemoglobin in solution at atomic resolution. Chemical Reviews 104: 1219–1230. https://doi.org/10.1021/cr940325w PMID: 15008621
28. Yuan Y, Tam MF, Simplaceanu V, Ho C (2015) New look at hemoglobin allostery. Chemical Reviews 115: 1702–1724. https://doi.org/10.1021/cr500495x PMID: 25607981
29. Rollema HS, Bauer C (1979) Interaction of inositol pentaphosphate with the hemoglobins of highland and lowland geese. Journal of Biological Chemistry 254: 2038–2043.
30. Oberthur W, Braunitzer G, Wurdinger I (1982) Hemoglobins of the bar-headed goose (*Anser indicus*)—primary structure and physiology of respiration, systematics and evolution. Hoppe-Seylers Zeitschrift Fur Physiologische Chemie 363: 581–590.
31. McCracken KG, Barger CP, Sorenson MD (2010) Phylogenetic and structural analysis of the HbA (α(A)/β(A)) and HbD (α(D)/β(A)) hemoglobin genes in two high-altitude waterfowl from the Himalayas and the Andes: bar-headed goose (*Anser indicus*) and Andean goose (*Chloephaga melanoptera*). Molecular Phylogenetics and Evolution 56: 649–658. https://doi.org/10.1016/j.ympev.2010.04.034 PMID: 20434566
32. Perutz MF (1983) Species adaptation in a protein molecule. Molecular Biology and Evolution 1: 1–28. https://doi.org/10.1093/oxfordjournals.molbev.a040299 PMID: 6400645
33. Jessen TH, Weber RE, Fermi G, Tame J, Braunitzer G (1991) Adaptation of bird hemoglobins to high-altitudes—demonstration of molecular mechanism by protein engineering. Proceedings of the National Academy of Sciences of the United States of America 88: 6519–6522. PMID: 1862080
34. Weber RE, Jessen TH, Malte H, Tame J (1993) Mutant hemoglobins (α(119)-Ala and β(55)-Ser)—functions related to high-altitude respiration in geese. Journal of Applied Physiology 75: 2646–2655. https://doi.org/10.1152/jappl.1993.75.6.2646 PMID: 8125885
35. Li W-H (1997) Molecular Evolution. Sunderland, MA: Sinauer Associates, Inc.
36. Hochachka PW, Somero GN (2002) Biochemical Adaptation. Oxford: Oxford University Press.
37. Harms MJ, Thornton JW (2010) Analyzing protein structure and function using ancestral gene reconstruction. Current Opinion in Structural Biology 20: 360–366. https://doi.org/10.1016/j.sbi.2010.03.005 PMID: 20413295
38. Hochberg GKA, Thornton JW (2017) Reconstructing ancient proteins to understand the causes of structure and function. Annual Review of Biophysics, 46: 247–269. https://doi.org/10.1146/annurev-biophys-070816-033631 PMID: 28301769
39. Gillespie JH (1991) The Causes of Molecular Evolution. New York: Oxford University Press.
40. Liang YH, Hua ZQ, Liang X, Xu Q, Lu GY (2001) The crystal structure of bar-headed goose hemoglobin in deoxy form: The allosteric mechanism of a hemoglobin species with high oxygen affinity. Journal of Molecular Biology 313: 123–137. https://doi.org/10.1006/jmbi.2001.5028 PMID: 11601851
41. Olson JS, Mathews AJ, Rohlfs RJ, Springer BA, Egeberg KD, et al. (1988) The role of the distal histidine in myoglobin and hemoglobin. Nature 336: 265–266. https://doi.org/10.1038/336265a0 PMID: 3057383
42. Mathews AJ, Rohlfs RJ, Olson JS, Tame J, Renaud JP, et al. (1989) The effects of E7 and E11 mutations on the kinetics of ligand-binding to R-state human hemoglobin. Journal of Biological Chemistry 264: 16573–16583. PMID: 2777799
43. Rohlfs RJ, Mathews AJ, Carver TE, Olson JS, Springer BA, et al. (1990) The effects of amino acid substitution at position E7 (residue 64) on the kinetics of ligand-binding to sperm whale myoglobin. Journal of Biological Chemistry 265: 3168–3176. PMID: 2303446

44. Birukou I, Schweers RL, Olson JS (2010) Distal histidine stabilizes bound O_2 and acts as a gate for ligand entry in both subunits of adult human hemoglobin. Journal of Biological Chemistry 285: 8840–8854. https://doi.org/10.1074/jbc.M109.053934 PMID: 20080971

45. Yuan Y, Simplaceanu V, Ho NT, Ho C (2010) An investigation of the distal histidyl hydrogen bonds in oxyhemoglobin: effects of temperature, pH, and inositol hexaphosphate. Biochemistry 49: 10606–10615. https://doi.org/10.1021/bi100927p PMID: 21077639

46. Lukin JA, Simplaceanu V, Zou M, Ho NT, Ho C (2000) NMR reveals hydrogen bonds between oxygen and distal histidines in oxyhemoglobin. Proceedings of the National Academy of Sciences of the United States of America 97: 10354–10358. https://doi.org/10.1073/pnas.190254697 PMID: 10962034

47. DePristo MA, Weinreich DM, Hartl DL (2005) Missense meanderings in sequence space: A biophysical view of protein evolution. Nature Reviews Genetics 6: 678–687. https://doi.org/10.1038/nrg1672 PMID: 16074985

48. Tokuriki N, Stricher F, Serrano L, Tawfik DS (2008) How protein stability and new functions trade off. PloS Computational Biology 4: e1000002. https://doi.org/10.1371/journal.pcbi.1000002 PMID: 18463696

49. Tokuriki N, Jackson CJ, Afriat-Jurnou L, Wyganowski KT, Tang R, et al. (2012) Diminishing returns and tradeoffs constrain the laboratory optimization of an enzyme. Nature Communications 3: 1257. https://doi.org/10.1038/ncomms2246 PMID: 23212386

50. Harms MJ, Thornton JW (2013) Evolutionary biochemistry: revealing the historical and physical causes of protein properties. Nature Reviews Genetics 14: 559–571. https://doi.org/10.1038/nrg3540 PMID: 23864121

51. Olson JS, Maillett DH (2005) Designing recombinant hemoglobin for use as a blood substitute. In: Winslow RM, editor. Blood Substitutes. San Diego, CA: Academic Press.

52. Bellelli A, Brunori M, Miele AE, Panetta G, Vallone B (2006) The allosteric properties of hemoglobin: Insights from natural and site directed mutants. Current Protein and Peptide Science 7: 17–45. PMID: 16472167

53. Bonaventura C, Henkens R, Alayash AI, Banerjee S, Crumbliss AL (2013) Molecular controls of the oxygenation and redox reactions of hemoglobin. Antioxidants & Redox Signaling 18: 2298–2313.

54. Varnado CL, Mollan TL, Birukou I, Smith BJZ, Henderson DP, et al. (2013) Development of recombinant hemoglobin-based oxygen carriers. Antioxidants & Redox Signaling 18: 2314–2328.

55. Kumar A, Natarajan C, Moriyama H, Witt CC, Weber RE, et al. (2017) Stability-mediated epistasis restricts accessible mutational pathways in the functional evolution of avian hemoglobin. Molecular Biology and Evolution 34: 1240–1251. https://doi.org/10.1093/molbev/msx085 PMID: 28201714

56. Olson JS, Eich RF, Smith LP, Warren JJ, Knowles BC (1997) Protein engineering strategies for designing more stable hemoglobin-based blood substitutes. Artificial Cells Blood Substitutes and Immobilization Biotechnology 25: 227–241.

57. Kim HW, Shen TJ, Sun DP, Ho NT, Madrid M, et al. (1994) Restoring allosterism with compensatory mutations in hemoglobin. Proceedings of the National Academy of Sciences of the United States of America 91: 11547–11551. PMID: 7972099

58. Tam MF, Rice NW, Maillett DH, Simplaceanu V, Ho NT, et al. (2013) Autoxidation and oxygen binding properties of recombinant hemoglobins with substitutions at the αVal-62 or βVal-67 position of the distal heme pocket. Journal of Biological Chemistry 288: 25512–25521. https://doi.org/10.1074/jbc.M113.474841 PMID: 23867463

59. Egeberg KD, Springer BA, Sligar SG, Carver TE, Rohlfs RJ, et al. (1990) The role of Val68(11) in ligand-binding to sperm whale myoglobin. Journal of Biological Chemistry 265: 11788–11795. PMID: 2114403

60. Tame J, Shih DTB, Pagnier J, Fermi G, Nagai K (1991) Functional role of the distal valine (E11) residue of α subunits in human hemoglobin. Journal of Molecular Biology 218: 761–767. PMID: 2023247

61. Quillin ML, Li TS, Olson JS, Phillips GN, Dou Y, et al. (1995) Structural and functional effects of apolar mutations of the distal valine in myoglobin. Journal of Molecular Biology 245: 416–436. PMID: 7837273

62. Brantley RE, Smerdon SJ, Wilkinson AJ, Singleton EW, Olson JS (1993) The mechanism of autooxidation of myoglobin. Journal of Biological Chemistry 268: 6995–7010. PMID: 8463233

63. Steinberg MH, Nagel RL (2009) Unstable hemoglobins, hemoglobins with altered oxygen affinity, Hemoglobin M, and other variants of clinical and biological interest. In: Steinberg MH, Forget BG, Higgs DR, Weaterhall DJ, editors. Disorders of hemoglobin: genetics, pathophysiology, and clinical management 2nd edition. Cambridge, UK: Cambridge University Press.

64. Streisfeld MA, Rausher MD (2011) Population genetics, pleiotropy, and the preferential fixation of mutations during adaptive evolution. Evolution 65: 629–642. https://doi.org/10.1111/j.1558-5646.2010.01165.x PMID: 21054357

65. Shen TJ, Ho NT, Simplaceanu V, Zou M, Green BN, et al. (1993) Production of unmodified human adult hemoglobin in *Escherichia coli*. Proceedings of the National Academy of Sciences of the United States of America 90: 8108–8112. PMID: 8367471

66. Natarajan C, Jiang X, Fago A, Weber RE, Moriyama H, et al. (2011) Expression and purification of recombinant hemoglobin in *Escherichia coli*. PloS One 6: e20176. https://doi.org/10.1371/journal.pone.0020176 PMID: 21625463

67. Natarajan C, Inoguchi N, Weber RE, Fago A, Moriyama H, et al. (2013) Epistasis among adaptive mutations in deer mouse hemoglobin. Science 340: 1324–1327. https://doi.org/10.1126/science.1236862 PMID: 23766324

68. Projecto-Garcia J, Natarajan C, Moriyama H, Weber RE, Fago A, et al. (2013) Repeated elevational transitions in hemoglobin function during the evolution of Andean hummingbirds. Proceedings of the National Academy of Sciences of the United States of America 110: 20669–20674. https://doi.org/10.1073/pnas.1315456110 PMID: 24297909

69. Cheviron ZA, Natarajan C, Projecto-Garcia J, Eddy DK, Jones J, et al. (2014) Integrating evolutionary and functional tests of adaptive hypotheses: a case study of altitudinal differentiation in hemoglobin function in an Andean sparrow, *Zonotrichia capensis*. Molecular Biology and Evolution 31: 2948–2962. https://doi.org/10.1093/molbev/msu234 PMID: 25135942

70. Galen SC, Natarajan C, Moriyama H, Weber RE, Fago A, et al. (2015) Contribution of a mutational hotspot to adaptive changes in hemoglobin function in high-altitude Andean house wrens. Proceedings of the National Academy of Sciences of the United States of America 112: 13958–13963. https://doi.org/10.1073/pnas.1507300112 PMID: 26460028

71. Natarajan C, Projecto-Garcia J, Moriyama H, Weber RE, Munoz-Fuentes V, et al. (2015) Convergent evolution of hemoglobin function in high-altitude Andean waterfowl involves limited parallelism at the molecular sequence level. PLoS Genetics 11: e1005681. https://doi.org/10.1371/journal.pgen.1005681 PMID: 26637114

72. Tufts DM, Natarajan C, Revsbech IG, Projecto-Garcia J, Hoffman FG, et al. (2015) Epistasis constrains mutational pathways of hemoglobin adaptation in high-altitude pikas. Molecular Biology and Evolution 32: 287–298. https://doi.org/10.1093/molbev/msu311 PMID: 25415962

73. Natarajan C, Hoffmann FG, Weber RE, Fago A, Witt CC, et al. (2016) Predictable convergence in hemoglobin function has unpredictable molecular underpinnings. Science 354: 336–340. https://doi.org/10.1126/science.aaf9070 PMID: 27846568

74. Zhu X, Guan Y, Signore AV, Natarajan C, DuBay SG, et al. (2018) Divergent and parallel routes of biochemical adaptation in high-altitude passerine birds from the Qinghai-Tibet Plateau. Proceedings of National Academy of Sciences USA 115: 1865–1870.

75. Weber RE (1992) Use of ionic and zwitterionic (tris bistris and HEPES) buffers in studies on hemoglobin function. Journal of Applied Physiology 72: 1611–1615. https://doi.org/10.1152/jappl.1992.72.4.1611 PMID: 1592755

76. Grispo MT, Natarajan C, Projecto-Garcia J, Moriyama H, Weber RE, et al. (2012) Gene duplication and the evolution of hemoglobin isoform differentiation in birds. Journal of Biological Chemistry 287: 37647–37658. https://doi.org/10.1074/jbc.M112.375600 PMID: 22962007

77. Weber RE, Fago A, Malte H, Storz JF, Gorr TA (2013) Lack of conventional oxygen-linked proton and anion binding sites does not impair allosteric regulation of oxygen binding in dwarf caiman hemoglobin. American Journal of Physiology-Regulatory Integrative and Comparative Physiology 305: R300–R312.

78. Helbo S, Fago A (2012) Functional properties of myoglobins from five whale species with different diving capacities. Journal of Experimental Biology 215: 3403–3410. https://doi.org/10.1242/jeb.073726 PMID: 22693033

79. Emsley P, Lohkamp B, Scott WG, Cowtan K (2010) Features and development of Coot. Acta Crystallographica Section D-Biological Crystallography 66: 486–501.

80. Liu XZ, Li SL, Jing H, Liang YH, Hua ZQ, et al. (2001) Avian haemoglobins and structural basis of high affinity for oxygen: structure of bar-headed goose aquomet haemoglobin. Acta Crystallographica Section D-Biological Crystallography 57: 775–783.

81. Liang YH, Liu XZ, Liu SH, Lu GY (2001) The structure of greylag goose oxy haemoglobin: the roles of four mutations compared with bar-headed goose haemoglobin. Acta Crystallographica Section D-Biological Crystallography 57: 1850–1856.